

**MINERALOGY OF THORIUM-ENHANCED MATERIALS WITHIN THE SOUTH POLE-AITKEN BASIN: POSSIBLE TRACES OF THE LUNAR UPPER MANTLE.** D. P. Moriarty III<sup>1</sup>, R. N. Watkins<sup>2</sup>, S. N. Valencia<sup>1</sup>, J. D. Kendall<sup>3</sup>, and N. E. Petro<sup>1</sup>, <sup>1</sup>NASA GSFC, 8800 Greenbelt Rd., Greenbelt, MD 20771 [Daniel.P.Moriarty@NASA.gov], <sup>2</sup>Planetary Science Institute, 1700 E Fort Lowell Rd., Tucson, AZ 85719. <sup>3</sup>University of Maryland Baltimore County, Baltimore, MD 21250.

**Introduction:** The South Pole – Aitken Basin (SPA) is a vast (~2500 km), ancient impact structure on the lunar farside. Due to the large scale of the impact, SPA is modeled to have excavated and melted large volumes of mantle materials [*e.g.*, 1,2]. The basin interior exhibits distinctive mineralogical and geochemical signatures, reflecting the unique thermal, geophysical, and geological evolution of the basin [*e.g.*, 3-7]. The basin exhibits an unusual enhancement in thorium abundance, the origin of which is hotly debated [*e.g.*, 8-14].

Thorium is a key elemental tracer of igneous processes, including crystallization of the lunar mantle. Because Th is incompatible in common lunar mineral structures, it tends to concentrate in melts. Models of lunar magma ocean crystallization predict that the concentration of Th and other incompatible elements (*i.e.*, potassium, rare earth elements, and phosphorus, known collectively as KREEP) are concentrated by a factor of ~100 in the final liquids to crystallize [*e.g.*, 15,16]. This final liquid would crystallize to form a ~50 km layer constituting the uppermost mantle. The mineral assemblage of this layer is modeled to include ~30% orthopyroxene, ~20% clinopyroxene, ~40% anorthosite, and ~10% incompatible-rich oxides [16]. For comparison, this assemblage is similar to Apollo 17 basaltic slabs (70017,541 and 70035,193) characterized by the Lunar Rock and Mineral Characterization Consortium [17]. However, this assemblage is denser than the underlying mantle cumulates (primarily olivine and orthopyroxene) and therefore the mantle is thought to have undergone gravitational overturn [16,18].

Here, we integrate Lunar Prospector (LP) measurements of the Th abundance across SPA [19] with Moon Mineralogy Mapper (M<sup>3</sup>) hyperspectral data [20], Lunar Reconnaissance Orbiter Camera (LROC) Wide Angle Camera (WAC) images [21], and Lunar Orbiter Laser Altimeter (LOLA) topography [22] to assess the mineralogy and geology of Th-bearing lithologies across SPA. These analyses inform our understanding of the structure and evolution of the lunar mantle, and have important implications for planning future sample return missions.

**Thorium Distribution and Abundance:** The LP-measured Th distribution across SPA [19] is shown in Fig. 1A. Contour lines were derived for 0.5 ppm Th intervals, further revealing the fine-scale structure of the distribution. In general, enhanced Th >~ 3 ppm is

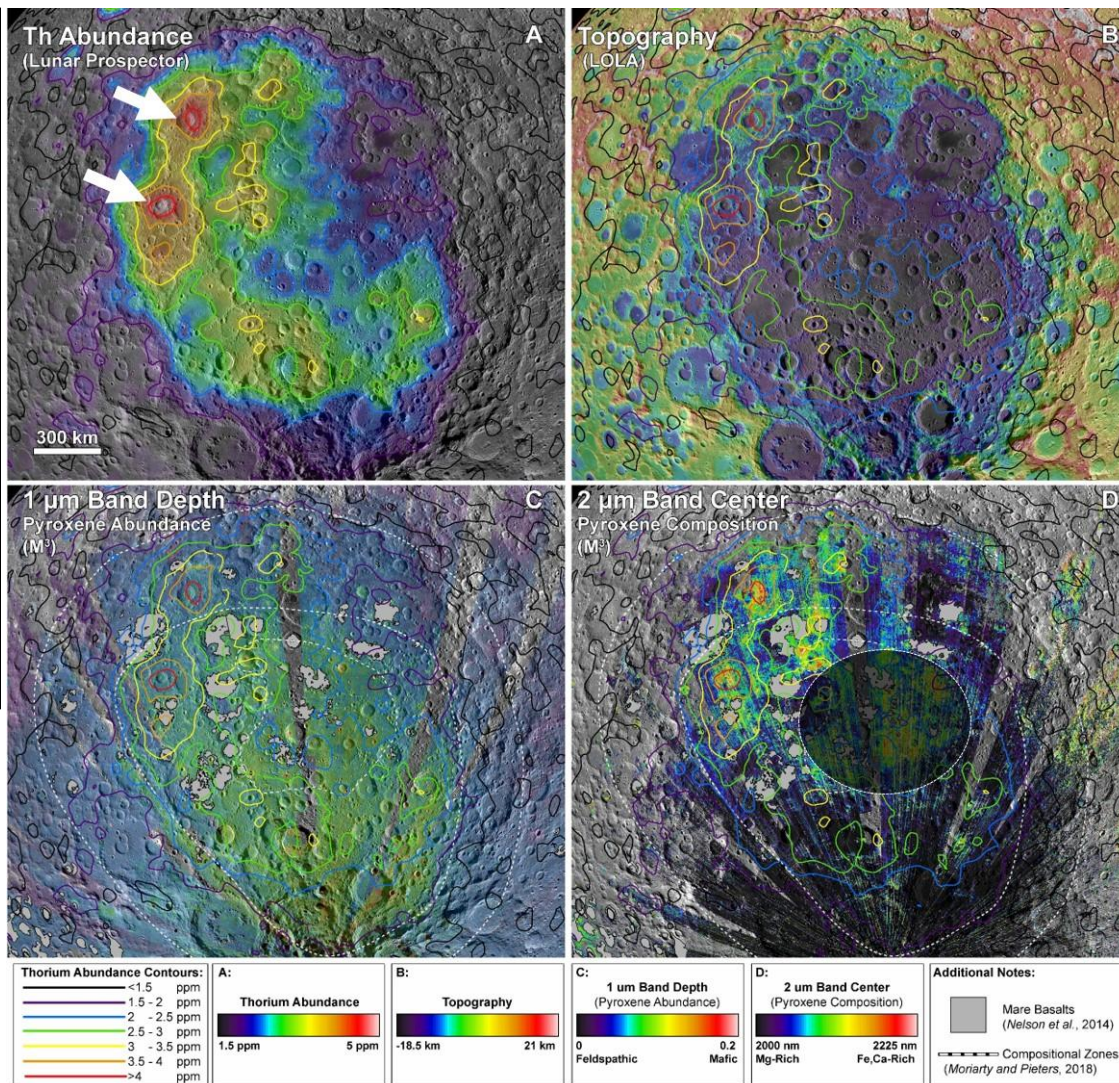
distributed in a crescent-shape pattern around western SPA. Local maxima in Th abundance are correlated with relatively young, large impact structures. This is especially apparent at Birkeland Crater (84 km, Eratosthenian) and Oresme V Crater (56 km, Upper Imbrian)[16]. These two craters are associated with Th “hotspots” and exhibit the highest Th abundance across SPA at ~5 ppm [19]. However, lower-magnitude local maxima are observed at several other young crater structures, including Finsen (73 km, Eratosthenian) and Rumford (61 km, Lower Imbrian)[23], marked by white arrows in Fig. 1A. Conversely, local Th minima are associated with resurfacing-related features such as mare basalts, Mafic Mound [6], and SPACA [7].

SPA impact models [1,2] suggest that a significant component (up to 50% or greater) of SPA ejecta originates from the uppermost mantle. Although the ejecta is modeled to be emplaced roughly symmetrically about impact trajectory angle [2], the mantle-derived ejecta would be diluted and modified by several processes, including: (A) mixing with SPA ejecta from the overlying crustal column [2], (B) mixing with target feldspathic crustal materials during ballistic ejecta emplacement and the SPA modification stage [*e.g.*, 24], (C) volcanic resurfacing (mare basalts, SPACA, Mafic Mound, etc.) [6,7], (D) emplacement of external basin ejecta [25], and (E) subsequent impact events either re-exposing SPA ejecta at the surface (Birkeland, Oresme V, Finsen, Rumford) or, in the case of basin-scale impacts, removing the ejecta blanket entirely (Apollo Basin, 524 km, Pre-Nectarian). Considering these processes, it is feasible that the observed Th distribution across SPA results from emplacement and subsequent evolution of Th-bearing SPA ejecta from the uppermost mantle [13].

**Mineralogical Properties of Th-Bearing Materials:** Assessing the mineralogy of Th-bearing materials across SPA enables insight into their origin. In addition to the overall correlation between Th abundance and surface mineralogy, the Th hotspots at Birkeland and Oresme V are of special interest, as they represent pristine exposures of Th-bearing materials within SPA.

Using the Parabolas and Linear Continua (PLC) spectral analysis technique [26], maps of compositionally-sensitive spectral parameters corresponding to pyroxene abundance and composition were derived from M<sup>3</sup> data. These maps are shown in Fig. 1C,D. In general, there is no obvious correlation between pyrox-

**Fig. 1:** (A) LP Th abundance [19]. Birkeland and Oresme V are indicated by white arrows. (B) LOLA topography [22]. (C) M<sup>3</sup>-derived 1-micron absorption band depth (correlated with pyroxene abundance). (D) M<sup>3</sup>-derived 2-micron absorption band center (correlated with pyroxene composition). Known mare basalts and SPACA have been masked. In all panels, the base-map is LROC WAC imagery [21], and 0.5 ppm Th contours have been superposed.



ene abundance and Th abundance. However, Th-bearing materials in the vicinity of Birkeland and Oresme V

are distinctive in terms of their pyroxene composition, as they exhibit relatively long-wavelength absorption bands indicating a basaltic composition. These spectral distinctions are especially pronounced in the walls and ejecta of Birkeland and Oresme V. While the Th-bearing materials do not exhibit a significantly higher pyroxene abundance than other local materials, the pyroxenes that are present are unusually basaltic relative to the low-Ca pyroxenes observed throughout most of SPA. These materials also exhibit lower albedos than typical non-mare materials.

**Conclusions:** The observed Th abundance across SPA is consistent with a SPA ejecta blanket modified by ~4 Ga of geologic evolution. The most pristine exposures of this material at Birkeland and Oresme V exhibit a basalt-like mineral assemblage. This is consistent with a Th-bearing, basalt-like uppermost mantle assemblage predicted from lunar magma ocean crystallization models [8,9], suggesting that the SPA-forming impact excavated a stratified, pre-overtturn upper man-

tle. Birkeland and Oresme V are the best locations to sample materials excavated from the uppermost mantle.

**Acknowledgements:** This work is supported through a NASA Postdoctoral Program Fellowship and SSERVI TREX #NNH16ZDA001N.

**References:** [1]Potter, RWK et al., (2012), *Icarus*, 220.2. [2] Melosh, HJ et al., (2017), *Geology*, 45. [3]Jolliff, BL et al., (2000), *JGR*, 105.E2. [4]Pieters, CM et al., (2001), *JGR*, 106.E11. [5]Ohtake, M et al., (2014), *GRL*, 41.8. [6]Moriarty, DP and Pieters, CM, (2015), *GRL*, 42.19. [7]Moriarty, DM and Pieters, CM, (2018), *JGR*, 123.3. [8]Stuart-Alexander, DE, (1978), *USGS Map I-1047*. [9]Haskin, LA et al., (1998), *MAPS*, 33. [10]Lawrence, DJ et al., (2000), *JGR*, 105. [11]Wieczorek, MA and Zuber, MT, (2001), *JGR*, 106. [12]Haskin, LA et al., (2004), *LPSC*, #1461. [13]Garrick-Bethell, I and Zuber, MT, (2005), *GRL*, 32. [14]Hagerty, JJ et al., (2011), *JGR*, 116. [15]Snyder, GA et al., (1992), *GCA*, 56.10. [16]Elkins-Tanton, LT et al., (2011), *EPSL*, 304.3-4. [17] Isaacson, PJ et al., (2011), *MAPS*, 46. [18]Hess, PC and Parmentier, EM, (1995), *EPSL*, 134.3-4. [19]Lawrence, DJ et al., (2007), *GRL*, 34.3. [20]Pieters, CM et al., (2009), *Current Sci*. [21]Robinson, MS et al., (2010), *SSR*, 150.1-4. [22]Smith, DE et al., (2010), *GRL*, 37.18. [23]Wilhelms, DE et al., (1987), *Geol. Hist. Moon*. [24]Osinski, GR et al., (2011), *EPSL*, 310.3-4. [25]Petro, NE and Pieters, CM, (2008), *MAPS*, 43.9. [26] Moriarty, DP and Pieters, CM, (2016), *MAPS*, 51.2.